J Solid State Electrochem (2010) 14:1667–1673
DOI 10.1007/s10008-009-0997-9

ORIGINAL PAPER

The electrochemical reduction reaction of dissolved oxygen on Q235 carbon steel in alkaline solution containing chloride ions

Yongjuan Li · Jiajia Wu · Dun Zhang · Yi Wang · Baorong Hou

Received: 28 September 2009 / Revised: 17 December 2009 / Accepted: 25 December 2009 / Published online: 9 February 2010
© Springer-Verlag 2010

Abstract Cyclic voltammetry, electrochemical impedance spectroscopy, and rotating disk electrode voltammetry have been used to study the effect of chloride ions on the dissolved oxygen reduction reaction (ORR) on Q235 carbon steel electrode in a 0.02 M calcium hydroxide ($Ca(OH)_2$) solutions imitating the liquid phase in concrete pores. The results indicate that the cathodic process on Q235 carbon steel electrode in oxygen-saturated 0.02 M $Ca(OH)_2$ with different concentrations of chloride ions contain three reactions except hydrogen evolution: dissolved oxygen reduction, the reduction of Fe(III) to Fe(II), and then the reduction of Fe(II) to Fe. The peak potential of ORR shifts to the positive direction as the chloride ion concentration increases. The oxygen molecule adsorption can be inhibited by the chloride ion adsorption, and the rate of ORR decreases as the concentration of chloride ions increases. The mechanism of ORR is changed from $2e^-$ and $4e^-$ reactions, occurring simultaneously, to quietly $4e^-$ reaction with the increasing chloride ion concentration.

Keywords Dissolved oxygen reduction reaction · Q235 carbon steel · Chloride ion · Cyclic voltammetry · Electrochemical impedance spectroscopy · Rotating disk electrode

Y. Li · J. Wu · D. Zhang (✉) · Y. Wang · B. Hou
Chinese Academy of Sciences, Institute of Oceanology,
7 Nanhai Road,
Qingdao 266071, China
e-mail: zhangdun@ms.qdio.ac.cn

Y. Li
College of Science, Gansu Agriculture University,
No. 1 Yingmen Village,
Lanzhou 730070, China

Introduction

As an important structure material, steel reinforced concrete has been widely used and plays a significant role in social and economic development. The protective oxide passive film is usually generated on the surface of steel reinforcement in the alkaline pore solution of concrete with a pH from 12.5 to 13.5. However, the oxide passive film will be destroyed due to the ingress of chloride ions, which can induce the localized corrosion of reinforcing steel [1–7].

Corrosion of reinforcing steel has been recognized as a serious problem which results in large economic consequences [8]. Chloride ions are a predominate element resulting in the corrosion of steel reinforcement since they attack the passivated steel by formation of an iron (Fe) oxide/hydroxide layer [7], which may be contributed by the concrete mixture ingredients or diffuse from deicing salts or marine environments. The mechanism of breakdown of the passive film has been studied by many authors [9–12]. Montemor [13] has presented an overview on the state of the art of the most important aspects of the corrosion process initiated by chlorides, its development, and monitoring techniques. The composition of the passive film formed on reinforcing steel and the mechanism of its breakdown by chlorides can be explained by more than one model. It can be assumed that chloride ion form soluble complexes with iron leading to localized acidification and consequent pit growth. In a word, the passive film destruction can result in the change of the steel from passivation to activation. The main cathodic reaction during the process of depassivation is dissolved oxygen reduction reaction (ORR) on surrounding passive steel [14].

The role of dissolved oxygen on rebar corrosion has been studied extensively [15–19]. Raupach [15, 16] studied the influence of dissolved oxygen on corrosion of steel in

degradation concrete and pointed out that the diffusion of oxygen was a significant limiting factor for the corrosion rate when the concrete around the reinforcement was water-saturated and most of the oxygen within the concrete near the reinforcement had been consumed by the cathodic reaction of the corrosion process. The corrosion rate is influenced by oxygen diffusion through the concrete cover in structures which are submerged or exposed to long-term or cyclic water application. Wang [17] investigated steel corrosion in sands cell with pore water for the simulation study on embedded-in-concrete steel in seawater and found that the steel corrosion was controlled by ORR. The water content and sand granularity could affect the corrosion behavior greatly. The corrosion rate of iron in a pH 10 solution of calcium hydroxide ($Ca(OH)_2$) containing 0.01 M sodium chloride (NaCl) was investigated by wet–dry cycles by Kim [18] and found that the large increase in the corrosion rate was induced by the acceleration of oxygen transport through the thin electrolyte layer. Sagues [19] studied the ORR on passive steel and Cr rich alloys for concrete reinforcement and found that the cathodic behavior under aeration reflected primarily oxygen reduction and not reduction of species in the passive film.

Q235 carbon steel is a kind of common construction steel which is used extensively in reinforced concrete constructions because of its preferable strength and fatigue resistance. However, as our knowledge, the effect of chloride ion on ORR on Q235 carbon steel in simulated concrete pore solution has not been reported.

The aim of present work is to study the electrochemistry reduction reaction of dissolved oxygen on Q235 carbon steel electrode in simulated concrete pore solutions containing chloride ions by cyclic voltammetry (CV), electrochemical impedance spectroscopy (EIS), and rotating disk electrode (RDE) voltammetry.

Experimental

Chemicals and materials

The elements with a mass percent of Q235 carbon steel are 0.1 C, 0.4 Mn, 0.12 Si, 0.02 S, and 0.05 P. Simulated concrete pore solutions with different NaCl concentrations were prepared by mixture of 0.02 M$Ca(OH)_2$ and 0.06, 0.1, and 0.6 MNaCl, respectively. Ultra-high purity nitrogen and oxygen gases (>99.999%, Qingdao Heli Gas Co., China) were fed to the electrochemical cells and used for the deaeration of solution and the preparation of oxygen-saturated solution, respectively. All reagents were analytical pure and purchased from Sinopharm Chemical Reagent Co., Ltd., China and the used water was Milli-Q water. The kinematic viscosity (ν) measured by an Ubbelohde viscometer in a thermostated water bath at 25 ± 0.1 °C of 0.02 M $Ca(OH)_2$ containing 0.06, 0.1, and 0.6 MNaCl was as 0.00898, 0.00906, and 0.00927 cm^2s^{-1}, respectively. In order to minimize atmospheric carbon dioxide contamination, the fresh solution was used during the kinematic viscosity measurement.

The Q235 carbon steel disk electrode (5 mm diameter) which was used in CV, EIS, and RDE measurement was sealed into epoxy resin. Prior to each experiment, the Q235 carbon steel disk electrode was polished orderly with No. 400, 800, 1,200, 3,000, and 5,000 silicon carbide paper and then was polished with 1 μm alumina powder. Finally, the electrode was ultrasonic cleaned in Milli-Q water for 10 min.

Electrochemical measurements

The electrochemical experiments were carried out by a computer-controlled electrochemical system (CHI 760C) with a three-electrode one-compartment electrochemical cell. The Q235 carbon steel disk electrode was used as working electrode. A silver/silver chloride (3 M potassium chloride) and a platinum wire electrode (CH Instruments, Inc.) were used as reference and counter electrode, respectively. A motor speed controller (Pine Research Instrument, Inc.) was used to control the rotating rate of electrode for RDE measurement.

The potential range of CV was from free corrosion potential to the hydrogen evolution potential. EIS was performed during the frequency of 0.05–10^5Hz with amplitude of 5 mV. RDE electrochemical experiment was recorded in nitrogen-saturated and oxygen-saturated 0.02 M$Ca(OH)_2$ containing 0.06, 0.1, and 0.6 MNaCl solutions at different rotating speeds. The Q235 carbon steel electrode was pretreated by soaking in air-saturated electrolytic solution for more than 30 min. In this paper, all potentials were referred to Ag/AgCl (3 MKCl) electrode. All electrochemical experiments were performed at 25 ± 2 °C.

Results and discussion

Cyclic voltammetry

Figure 1 shows the plots of cyclic voltammograms obtained on Q235 carbon steel electrode in nitrogen-saturated and oxygen-saturated 0.02 M$Ca(OH)_2$ solutions containing 0.06 (a), 0.1 (b), and 0.6 M (c)NaCl. Except the hydrogen evolution at the potential more negative than −1.20 V, there are two principal reduction peaks (peak I' and II') observed at the potentials of −1.15 and −0.93 V in nitrogen-saturated solution (curve a in Fig. 1a), which can be attributed to the reduction of ferrous oxide to iron (Eq. 2) and the reduction

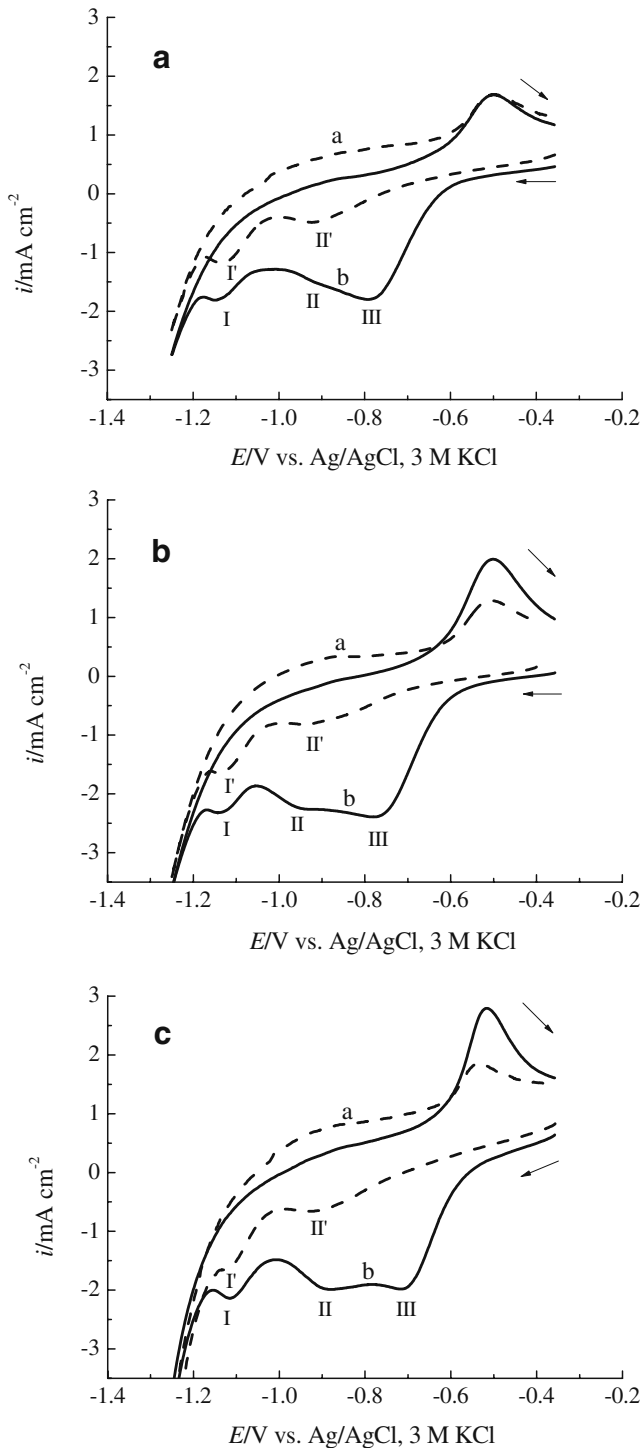

Fig. 1 Cyclic voltammograms obtained on Q235 carbon steel electrode in nitrogen-saturated (a) and oxygen-saturated (b) 0.02 M$Ca(OH)_2$ solutions containing 0.06 (**a**), 0.1 (**b**), and 0.6 M (**c**)NaCl at a scan rate of 0.1 Vs^{-1}. The *arrows* indicate the direction of scan potential

of ferric oxide to ferrous oxide (Eq. 1) on the carbon steel electrode, respectively [20, 21].

$$Fe^{3+} + e^- \rightarrow Fe^{2+} \quad (1)$$

$$Fe^{2+} + 2e^- \rightarrow Fe \quad (2)$$

Table 1 The pH values, the peak potentials of ORR (E_P^{ORR}), and the open-circuit potential (E_{oc}) in oxygen-saturated 0.02 M$Ca(OH)_2$ solutions containing different concentrations of chloride ions

$[Cl^{-1}]$ (M)	0.06	0.1	0.6
pH	12.84	12.74	12.59
E_P^{ORR} (V)	−0.80	−0.75	−0.70
E_{oc} (V)	−0.33	−0.38	−0.45

Except these two reduction peaks (peak I and II), another reduction peak (peak III) appears at the potential of −0.8 V in oxygen-saturated solution (curve b in Fig. 1a), indicating that the ORR occurs on the Q235 carbon steel electrode. However, peak II and peak III cannot be separated clearly. As increasing the chloride ion concentration, the separation of these two peaks (peak II and III) becomes clearer (curve b in Fig. 1b and c) and the peak potential of ORR shifts to more positive direction. The pH values and the peak potentials of ORR in 0.02 M$Ca(OH)_2$ solutions containing different chloride ion concentrations were listed in Table 1. It can be observed obviously in Table 1 that the pH value decreases with the increasing of the concentration of chloride ions. According to the Nernst equation (Eq. 3), the relationship between φ_{O_2/H_2O} and pH at 25 °C can be given in Eq. 4.

$$\varphi_{O_2/H_2O} = \varphi_{O_2/H_2O}{}^0 + \frac{2.303RT}{nF} \lg\left(P_{O_2}\alpha_{H^+}^4\right) \quad (3)$$

$$\varphi_{O_2/H_2O} = 1.23 - 0.0592pH \quad (4)$$

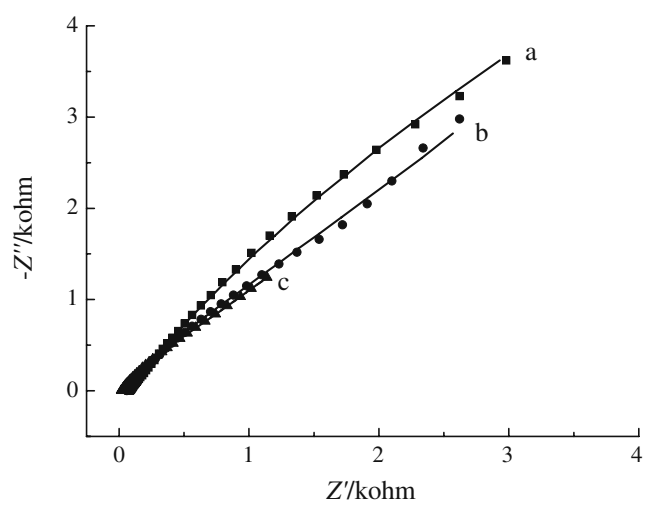

Fig. 2 Nyquist plots obtained on Q235 carbon steel electrode in oxygen-saturated 0.02 M$Ca(OH)_2$ solutions containing 0.06 (a), 0.1 (b), and 0.6 M (c) NaCl at ORR peak potentials of −0.80, −0.75, and −0.70 V, respectively. (*Symbol*: the experimental data; *curve*: the fit curve)

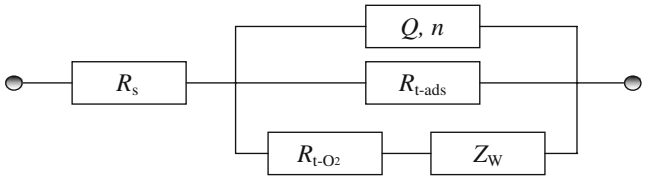

Fig. 3 The schematic illustration of the equivalent circuit

Based on Eq. 4, the decrease of pH value will induce the positive shift of the reaction potential, which can explain that the peak potential of ORR shifts to the positive direction as decreasing pH value. What's more, compared to the reduction of ferrous oxide, the ORR is more sensitive to the pH, which can help to explain that the peak II and peak III separates more clearly as decreasing the pH value.

It can be observed in Fig. 1 that the anodic reaction peak currents also increase along with the increasing of the chloride ion concentration, which can be attributed to that the protective film formed in a high pH solution can be kept in the low concentration of chloride ion, and as increasing the chloride ion concentration, this protective film will be destroyed and the oxygen can easily reach at the surface of carbon steel which can strength the oxidation of iron.

Electrochemical impedance spectroscopy

In our previous study, EIS has been successfully used to investigate the mechanism of ORR on the glassy carbon electrode in 3.5% NaCl solution [22]. In this work, EIS measurement in the frequency range from 10^5 Hz down to 0.05 Hz has been performed systematically at the Q235 carbon steel electrode.

The experimental impedance spectra in different chloride ion concentrations are shown in Fig. 2 (symbol) and the fitting curves according to the equivalent circuit (Fig. 3) are shown in Fig. 2 (curve). The potential was selected nearly the peak potential of the ORR as −0.80, −0.75, and −0.70 V in the solutions containing 0.06 (a), 0.1 (b), and 0.6 M (c) NaCl, respectively. At these potentials, the ORR process makes the main contribution to the electrochemical reaction. The ORR is a complicated process involving many elementary reactions that may generate various intermediate reactive oxygen species and strongly influences the electrode surface state and the adsorption of the anions [23]. Therefore, the equivalent circuit for the EIS is expressed and shown in Fig. 3. In the circuit, R_s represents solution resistance. Q is a constant phase element substituting for the capacitive element to give a more accurate fit and its admittance and impedance are expressed as:

$$Y = Y^0(j\omega)^m \tag{5}$$

$$Z = \frac{1}{Y^0}(j\omega)^{-m} \tag{6}$$

Where Y^0 is the magnitude of Q, ω is the angular frequency, and m is the exponential term relating to the roughness of electrode surface. $R_{t\text{-}ads}$ is the charge-transfer resistance of further reduction of the adsorbed intermediates. $R_{t\text{-}O_2}$ is the charge-transfer resistance of the direct $2e^-/4e^-$ ORR from oxygen molecules. Z_W is the magnitude of the Warburg impedance.

The EIS parameters of Q235 carbon steel electrode at the peak potentials of ORR in oxygen-saturated 0.02 MCa $(OH)_2$ solution with different chloride ion concentrations were listed in Table 2. It can be observed in Table 2 that the R_s decreases with the increasing of chloride ion concentration, which can be attributed that the conductivity of solution increases as the increasing of the ion concentration. The reaction resistance of oxygen molecule in series with the Warburg impedance and the reaction resistance of adsorbed substance are connected in parallel, while the value of $R_{t\text{-}O_2}$ is far lower than that of $R_{t\text{-}ads}$, indicating that the oxygen molecule direct $2e^-/4e^-$ reduction reaction is a fast step and has more significant on the cathodic process. Moreover, the value of $R_{t\text{-}O_2}$ is one order of magnitude compared to that of Z_W when the chloride ion concentration is 0.06 M, and the value of $R_{t\text{-}O_2}$ is much larger than that of Z_W when the chloride ion concentrations are 0.1 and 0.6 M, indicating that the ORR is controlled by a mixed mass transfer and electron transfer process in simulated with a small amount of chloride ions and a electron transfer process with a large amount of chloride ions at test potential. The value of R_s decreases as the chloride ion concentration increases and the value of $R_{t\text{-}O_2}$ is, on the contrary, indicating that the adsorption of large amount of chloride ions can inhibit the coadsorption of oxygen molecules. Gojkovic [24] has proposed the adsorption

Table 2 Impedance parameters obtained on Q235 carbon steel electrode at the peak potentials of ORR in oxygen-saturated 0.02 MCa$(OH)_2$ solutions with different concentrations of chloride ions

$[Cl^{-1}]$ (M)	E (V)	R_s (Ωcm^2)	Y^0 (Fcm^{-2})	m	$R_{t\text{-}ads}$ (Ωcm^2)	$R_{t\text{-}O_2}$ (Ωcm^2)	Z_W (Ω cm^2)
0.06	−0.80	81.52	4.28E−4	0.6949	1.35E+07	1.41E+3	3.23E+3
0.1	−0.75	59.75	2.81E−4	0.7368	4.42E+09	2.03E+4	3.03E+3
0.6	−0.70	20.28	5.00E−4	0.7505	7.52E+10	1.08E+5	1.52E+3

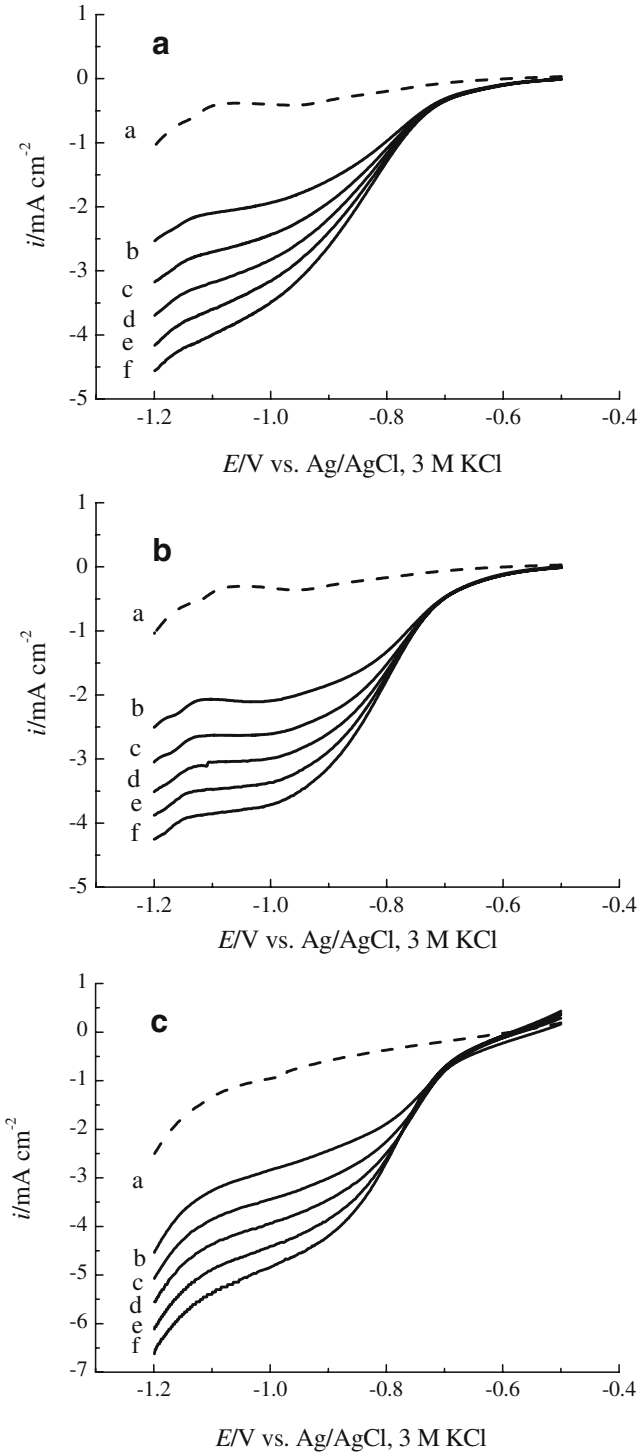

Fig. 4 RDE voltammograms obtained on Q235 carbon steel electrode in nitrogen-saturated (*line* a) and oxygen-saturated (*lines* b to f) 0.02 M $Ca(OH)_2$ solutions containing 0.06 (**a**), 0.1 (**b**), and 0.6 M (**c**) NaCl at a scan rate of 0.01 Vs^{-1} with a rotation rate of 200 (b), 400 (a and c), 600 (d), 800 (e), and 1,000 rpm (f)

theory of ORR mechanism and considered that the adsorption of oxygen molecules on $Fe(II)_{ox}$ surface sites acting as the active center was the ORR rate determining step. Many other scholars, such as Zecevic [25], Miyata [26], and Kear [27] also put forward that the adsorption-catalyzed process is included in ORR. Thus, the adsorption of chloride ions on the Q235 carbon steel electrode surface can inhibit the adsorption of oxygen molecules, which can

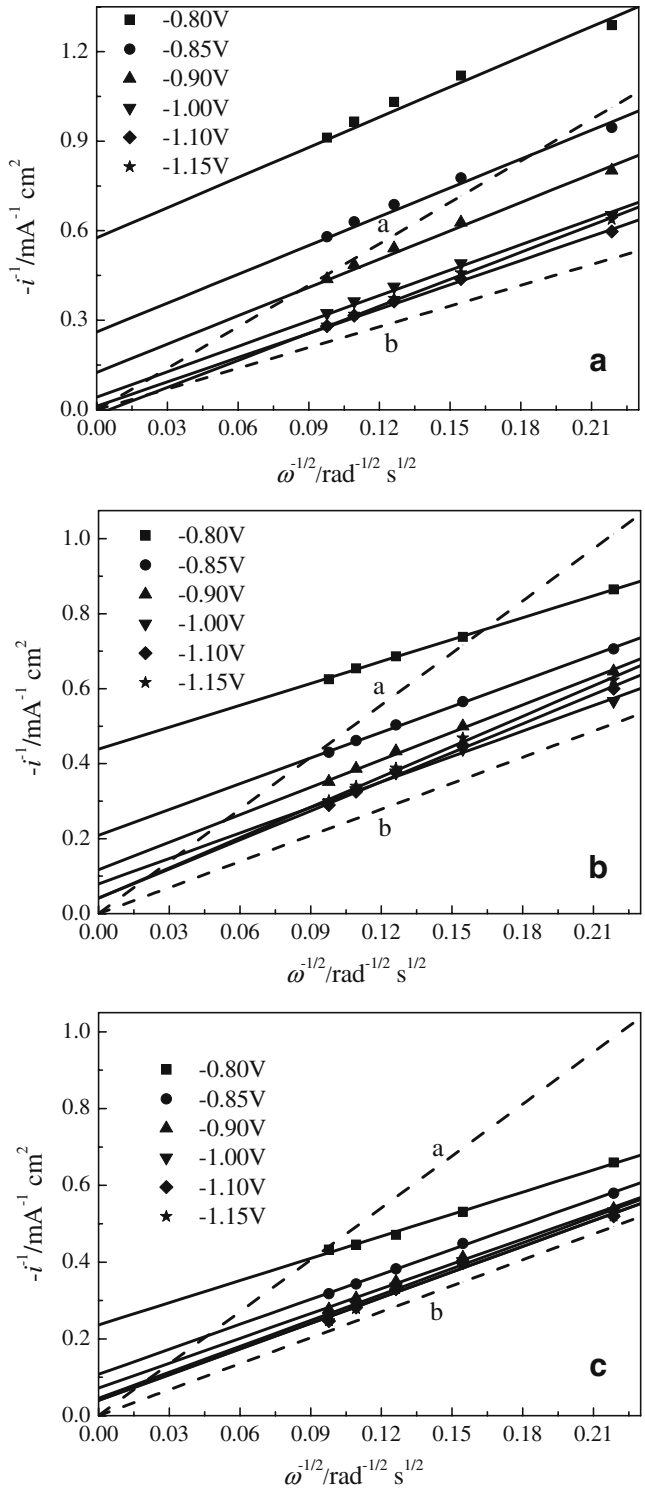

Fig. 5 Koutechý–Levich plots at different potentials in 0.02 M $Ca(OH)_2$ solutions containing 0.06 (**a**), 0.1 (**b**), and 0.6 M (**c**) NaCl. Data obtained from Fig. 4

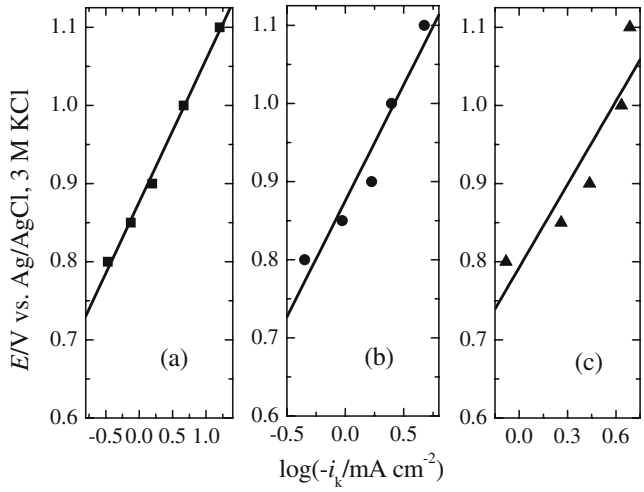

Fig. 6 The Tafel plots in 0.02 M$Ca(OH)_2$ solutions containing 0.06 M (**a**), 0.1 M (**b**), and 0.6 M (**c**) NaCl. Data obtained from Fig. 4

help to inhibit the breakage of O-O bond of oxygen molecules to decrease the rate of ORR.

Rotating disk electrode voltammetry

Figure 4 depicts the voltammograms obtained by the rotating disk electrode experiments at a scan rate of 0.01 Vs^{-1} at various electrode rotational rates in oxygen-saturated and nitrogen-saturated 0.02 M$Ca(OH)_2$ solutions containing 0.06, 0.1, and 0.6 MNaCl. It is evident that the curves obtained are expressed limiting plateau dependent on the rotation rate. The current obtained in oxygen-saturated solution increases as the rotation rate of the electrode increases and the limiting current for oxygen reduction appears at the potential range of -0.90 V to more negative direction. The limiting plateau and the dependence of the reduction current on rotation rate indicate that the process is under a mixed charge transfer and mass transfer control at all rotation rates.

To obtain the kinetics parameter on the number of transfer electron for ORR, $-i^{-1}$ vs. $\omega^{-1/2}$ curves were plotted in Fig. 5 according to the Koutecký–Levich equation (Eqs. 7 and 8).

$$\frac{1}{i} = \frac{1}{i_K} + \frac{1}{i_L} = \frac{1}{i_K} + \frac{1}{B\sqrt{\omega}} \tag{7}$$

$$B = 0.62nFC_{O_2}D^{2/3}v^{-1/6} \tag{8}$$

where i is the current density (A cm^{-2}); i_k is the kinetics current density (A cm^{-2}); i_L is the limiting current density (A cm^{-2}); n is the number of transfer electron; F is the Faraday constant (96,485 Cmol^{-1}); C_{O_2} is the concentration of oxygen in the solution (moles per cubic centimeter); D is the diffusion coefficient; ω is the rotation rate (rad per second). In this study, the values of C_{O_2} and D were cited as 1.18×10^{-3}M and $1.90 \times 10^{-5}cm^2s^{-1}$ [28] in simulated solutions with 0.06 M and 0.1 MNaCl. The values of C_{O_2} and D were cited as 0.938×10^{-3}M and $2.17 \times 10^{-5}cm^2s^{-1}$ [29] in simulated solution with 0.6 MNaCl.

The theoretical calculated lines of $2e^-$ and $4e^-$ transfer reactions are presented in Fig. 5 by the dash lines a and b. It is evidently that the ORR at −0.80 and −0.85 V is weak linear in the 0.06 MNaCl solution, indicating that the ORR at this potential range is mixed-control process. However, at the potentials more negative than −0.85 V, the ORR is completely mass transferred-control process. The slopes of the lines are between the $2e^-$ and $4e^-$. This fairly good agreement between the experimental and calculated values indicates that a $2e^-$ and $4e^-$ reduction reactions takes place simultaneously.

When the chloride ion concentration increases, we can find that the slopes of the lines are almost exactly on the theoretical $4e^-$ reaction line, which indicates that a $4e^-$ reduction takes place. This means that in the region of high current densities oxygen is probably completely reduced to OH^{-1}. According to the literature, the corrosion products on the surface of carbon steel are mainly α-FeOOH and γ-FeOOH without chloride ions [30–32], whereas when a large amount of chloride ions were present in the solution, the β-FeOOH as the main phase tend to increase and results in thicker film [33–35]. The different formation of iron oxide may cause the change of ORR mechanism. However, it is unlucky that the detail mechanism is still unknown. Thus, the relative studies on this topic are carried out in our group.

According to Eqs. 7 and 8, the dynamic current i_k can be obtained from the intercept of Fig. 5. To obtain further information on the kinetics parameters of ORR, log(i_k) vs. E curves were plotted in Fig. 6. It can be observed in Fig. 6 that the logarithm of i_k is linearly correlated with E, namely it is according with the Tafel equation (Eq. 9) [36].

$$\eta = \frac{2.303RT}{\alpha nF}(\log i_0 - \log i_k) \tag{9}$$

Table 3 The kinetics parameters of ORR obtained on Q235 carbon steel electrode in oxygen-saturated 0.02 M$Ca(OH)_2$ solutions with different concentrations of chloride ions

$[Cl^-]$ (M)	i_k (μAcm^{-2})	α	10^5k_0 (cms^{-1})	Tafel slope (mVdec^{-1})
0.06	−4.70	0.69	5.02	213
0.1	−3.36	0.50	4.15	297
0.6	−2.82	0.42	3.15	354

where η is the over potential (V) and can be calculated from Eq. 10; the intercept and slope can be indicated as Eqs. 11 and 12; i_0 is the reaction current density (A cm^{-2}); i_k is the kinetics current density (A cm^{-2}); n is the number of transfer electron; α is transfer coefficient; F is the Faraday constant (96,485 Cmol^{-1}).

$$\eta = E - E^0 \tag{10}$$

$$\text{Tafel slope} = \frac{2.303\mathrm{R}T}{\alpha nF} \tag{11}$$

$$\text{Intercept} = \frac{2.303\mathrm{R}T}{\alpha nF}\log i_0 \tag{12}$$

According to Tafel equation (Eq. 10), When $\eta = 0$ and $i_0 = i_k$, the standard rate constants k^0 can be determined from Eq. 13.

$$i_0 = nFck^0 \tag{13}$$

The values of k^0 and Tafel slopes were determined and listed in Table 3. It can be observed in Table 3 that the value of k^0 decreases and the Tafel slope increases as the chloride ion concentration increases, which is consistent with the results of EIS that the $R_{t\text{-}O_2}$ increases as the chloride ion concentration increases. This result further proves that the ORR is inhibited by the presence of chloride ion.

Conclusions

The work described in this paper presented that the cathodic process on Q235 carbon steel electrode in oxygen-saturated simulated concrete pore solutions with different chloride ion concentrations contains three reactions except hydrogen evolution: the reduction of dissolved oxygen, the reduction of Fe(III) to Fe(II), and then the further reduction of Fe(II) to Fe. The increase of the chloride ion concentration, which can decrease the pH of the simulated concrete pore solution, makes the peak potential of ORR shift to the positive direction and the over potential decrease. The EIS and RDE voltammetry investigations show that the oxygen molecule adsorption is inhibited by the chloride ion adsorption. What's more is that as the chloride ion concentration increases, the rate of ORR decreases and the mechanism of ORR changes from $2e^-$ and $4e^-$ reactions, occurring simultaneously, to quietly $4e^-$ reaction.

Acknowledgments This work was supported by National Natured Science Foundation of China (grant no. 40876041), Science and Technology Basic Research Program of Qingdao (grant no.09-1-3-16-jch) and National Key Technology R&D Program of China (grant 2007BAB27B01).

References

1. Moreno M, Morris W, Alvarez MG, Duffó GS (2004) Corros Sci 46:2681
2. Kumar V (1998) Corros Rev 16:317
3. Maslehuddin M, Al-Zahrani MM, Ibrahim M, Al-Mehthel MH, Al-Idi SH (2007) Constr Build Mater 21:1825
4. Du RG, Hu RG, Huang RS, Lin CJ (2006) Anal Chem 78:3179
5. Huet B, L'Hostis V, Miserque F, Idrissi H (2005) Electrochim Acta 51:172
6. Alonso C, Castellote M, Andrade C (2002) Electrochim Acta 47:3469
7. Pourbaix M (1974) Atlas of electrochemical equilibria in aqueous solutions. National Association of Corrosion Engineers, Houston
8. Ahmad S (2003) Cem Concr Compos 25:459
9. Jovancicevic V, Bockris JM, Carbajal JL, Zelenay P, Mizuno T (1986) J Electrochem Soc 133:2219
10. Saremi M, Mahallati E (2002) Cem Concr Res 32:1915
11. Pou TE, Murphy OJ, Young V, Bockris JOM, Tangson LL (1984) J Electrochem Soc 131:1243
12. Glass GK, Buenfeld NR (1997) Corros Sci 39:1001
13. Montemor MF, Simoes AMP, Ferreira MGS (2003) Cem concr compos 25:491
14. Sagues AA, Pech-Canul MA, Al-Mansur AKM (2003) Corros Sci 45:7
15. Raupach M (1996) Mater Struct 29:174
16. Raupach M (1996) Mater Struct 29:226
17. Wang J (1997) Chin J Oceanol Limnol 15:369
18. Kim JK, Nishikata A, Tsuru T (2003) Matrt trans 44:396
19. Sagues AA, Virtanen S, Schmuki P (2006) In: Marcus P, Maurice V (eds) Proceedings of the international conference on passivation of metals, and properties of thin oxide layers. Amsterdam, Elsevier
20. Baek WC, Kang T, Sohn HJ, Kho YT (2001) Electrochim Acta 46:2321
21. Joiret S, Keddam M, Nóvoa XR, Pérez MC, Rangel C, Takenouti H (2002) Cem Concr Compos 24:7
22. Kuang F, Zhang D, Li YJ, Wan Y, Hou BR (2009) J Solid State Electrochem 13:385
23. Lu YH, Xu HB, Wang J, Kong XF (2009) Electrochim Acta 54:3972
24. Gojkovićč SLJ, Zečević SK, Dražić DM (1994) Electrochim Acta 39:975
25. Zečević SK, Dražić DM, Gojkovićč SLJ (1989) J Electroanal Chem 265:179
26. Miyata Y, Asakura S (2002) Corros Sci 44:589
27. Kear G, Barker BD, Walsh FC (2004) Corrosion 60:561
28. Tammeveski K, Arulepp M, Tenno T, Ferrater C, Claret J (1997) Electrochim Acta 42:2961
29. Gojkovićč SLJ, Zečević SK, Obradović MD, Dražić DM (1998) Corros Sci 40:849
30. Duffó GS, Morris W, Raspini I, Saragovi C (2004) Corros Sci 46:2143
31. Hœrlé S, Mazaudier F, Dillmann Ph, Santarini G (2004) Corros Sci 46:1431
32. Antony H, Legrand L, Maréchal L, Perrin S, Dillmann Ph, Chaussé A (2005) Electrochim Acta 51:745
33. Nishimura T, Katayama H, Noda K, Kodama T (2000) Corrosion 56:935
34. Chitty W-J, Dillmann Ph, L'Hostis V, Lombard C (2005) Corros Sci 47:1555
35. Montemor MF, Simoes AMP, Ferreira MGS (1998) Corrosion 54:347
36. Zhang XD, Li WS, Huang YJ, Peng HY (2008) Acta Phys-Chim Sin 24:69